

Imaging erythrocytes under physiological conditions by atomic force microscopy

Robert Nowakowski^{a,1}, Paul Luckham^{a,*}, Peter Winlove^{b,2}

^a *Department of Chemical Engineering and Chemical Technology, Imperial College of Science, Technology and Medicine, Prince Consort Road, London SW7 2BY, UK*

^b *Physiological Flow Studies Laboratory, Imperial College of Science, Technology and Medicine, Prince Consort Road, London SW7 2BY, UK*

Received 15 March 2001; received in revised form 5 June 2001; accepted 11 June 2001

Abstract

Since its invention in the mid 1980s atomic force microscopy has revolutionised the way in which surfaces can be imaged. Close to atomic resolution has been achieved for some materials and numerous images of molecules on surfaces have been recorded. Atomic force microscopy has also been of benefit to biology where protein molecules on surfaces have been studied and even whole cells have been investigated. Here we report a study of red blood cells which have been imaged in a physiological medium. At high resolution, the underlying cytoskeleton of the blood cell has been resolved and flaws in the cytoskeleton structure may be observed. Comparison of the normal ‘doughnut’ shaped cells with swollen cells has been undertaken. Differences in both the global properties of the cells and in the local features in cytoskeleton structure have been observed. © 2001 Elsevier Science B.V. All rights reserved.

Keywords: Erythrocyte membrane; Atomic force microscopy; AFM; Spectrin

1. Introduction

Atomic force microscopy (AFM) has been widely applied in imaging biological materials in both air and in liquid (physiological) environments. Fixed cells were the first biological specimens imaged by this technique [1,2]. From these papers the advantage

of AFM as an instrument which can provide high resolution images of cell surfaces under native conditions has been demonstrated. On the other hand the difficulties and limitations specially in the study of soft mammalian cells have been noticed. In particular, the resolution obtained is far from molecular, the reason for this mainly results from tip-induced deformation of the soft cell surface. Nowadays, application of AFM to the imaging of cells is of great interest and progress has been summarised in recent reviews [3–6]. The utility of AFM strongly varies depending on the cell type, its wall structure and adhesion property. In some cases a resolution of about 10 nm has been achieved. This level of resolution has enabled the surface morphology of mammalian cells to be studied, for example: glial cells [7], rat

* Corresponding author. Fax: +44-171-594-5604.

E-mail address: p.luckham01@ic.ac.uk (P. Luckham).

¹ Present address: Institute of Physical Chemistry, Polish Academy of Sciences, Kasprzaka str. 44/52, Warsaw 01-224, Poland.

² Present address: School of Physiology, University of Exeter, Exeter EX4 4QL, Devon, UK.

leukaemic mast cells RBL-2H3 [8,9] and Madin–Darby canine kidney cells MDCK [10].

The erythrocyte membrane is one of the most extensively studied cell membranes [11–16]. In order to achieve the desired flexibility, whilst retaining its normal biconcave shape, the erythrocyte membrane contains a cytoskeleton which lies underneath the plasma membrane. One of the most commonly used techniques to study the cytoskeleton has been electron microscopy. However, a significant disadvantage of this method is that only highly processed cells (dry and usually only replicated samples) can be studied.

In early AFM work, images of fixed erythrocytes were presented [1,2]. Easily recognisable erythrocytes were observed but little subcellular detail was seen. However, imaging at high resolution for erythrocytes is difficult to achieve due to the approximate spherical shape and high flexibility of the cells. Häberle et al. [17] studied erythrocytes using a modified AFM. In this method the separated cell was immobilised on a micropipette which was mounted on the scanner. The imaging was performed on the protruding part of the cell. This elegant method has several advantages. One is resolution, which was in the 10 nm range. However, the major disadvantage is the complex instrumentation which is technically difficult to set up. Recently Mikrut and MacDonald [18] published results using a standard AFM system (Explorer, TopoMetrix, CA, USA). Both whole cell and cytoskeletal network have been imaged. However, in order to obtain the high resolution images of cytoskeletal network the cell was lysed with a low salt buffer and the haemoglobin rinsed away. In this way part of the cytoskeleton was imaged on the substrate in buffer solution. The likelihood of artefacts was therefore considerable.

Here we present our results concerning a study of the topography of erythrocytes, which have been obtained using standard AFM equipment. To ensure that the cells were close to the native condition scans were performed in physiological saline solution.

2. Materials and methods

The blood was obtained from Male Sprague–Dawley rats, anticoagulated with heparin and used immediately

after extraction. In order to visualise the blood cells with atomic force microscopy, the cells were attached to a glass surface. This was achieved by glutaraldehyde cross-linking poly-L-lysine to the glass surface. All the chemicals used (poly-L-lysine, phosphate buffered saline and glutaraldehyde) were purchased from Sigma (UK). Based on a method described [1] the following immobilisation procedure was applied. First, microscope coverslips were cleaned by means of standard surfactant and rinsed by distilled water. The coverslips were then dipped in a solution of poly-L-lysine (0.5 mg/ml), rinsed with a 1% aqueous glutaraldehyde solution and washed with phosphate buffered saline (PBS). The freshly extracted blood was then diluted in PBS (20 times) and this solution introduced to the treated glass surfaces and left to interact for 5 min. A 1% glutaraldehyde solution was then added again for 1 min to rigidify the cells. The cells were then washed with PBS and placed underneath a Topometrix Explorer AFM fitted with a standard or super silicon nitride AFM tips and a 150 μm scanner (all from TopoMetrix). All scans were performed at ambient temperature in PBS solution.

3. Results and discussion

Fig. 1 is a relatively low resolution image of several red blood cells. Depending on the location on the surface, both separated individual cells and self-organised monolayers of the tightly packed cells (on left side of the bottom of Fig. 1) may be observed. The thickness of the monolayer is around 2–3 μm , which corresponds to the total thickness of the individual cells. It may be seen that the vast majority of cells are the expected, biconcave (doughnut) shaped cells; however, at the top of Fig. 1 there are two cells which seem as though they are flat topped or spherical. It is possible to zoom in on an individual cell and such images are shown in Fig. 2 for both (A) the biconcave shaped cell and (B) a spherical cell. Comparison of the height profiles indicates that the swollen cells are higher (approx. 3 μm) than the biconcave ones (approx. 2 μm). The observed diameter of the cells is about 10 μm . This size is larger than the size of real cells and is due to an artefact. Note that the apparent slope on the sides of the cells are an

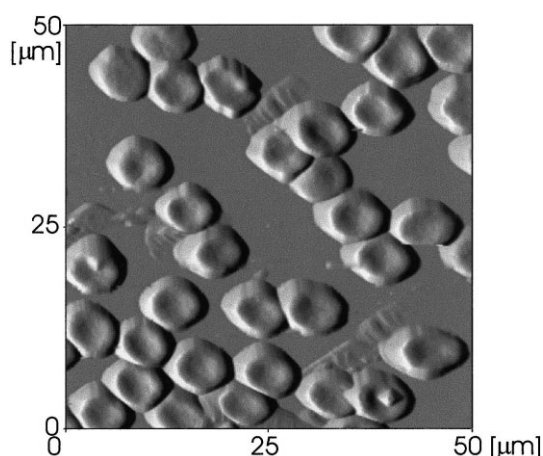


Fig. 1. AFM image of living erythrocytes on glass support obtained in PBS solution; scanning area $50 \times 50 \mu\text{m}^2$, max. height $3.4 \mu\text{m}$.

artefact and are due to the angle of the AFM tip used. This gives rise to the apparent diameter of the cells being larger than the real cells by $1\text{--}2 \mu\text{m}$. Similar artefacts due to the tip shape may also be seen in the bottom of the hollow on the biconcave shaped cell (Fig. 2A), where a triangular structure is seen. This is due to the triangular based pyramidal tip used. Careful inspection of the cells reveals a few 'dimples' on their surface which are much more common in the surfaces of the swollen form (Fig. 2B Fig. 3). It is likely that cells of this type are pathological, and that their cytoskeleton, i.e. the underlying pro-

tein structure in the cytoplasm of the cell, is weakened and hence the normal biconcave nature of the cell is changed for the thermodynamically more favourable spherical form.

High resolution images of erythrocytes are difficult to acquire, since erythrocytes are soft and deformable, the cell surface is elastic and the cells retain their three-dimensional shape when adsorbed to surfaces. In the case of erythrocytes high resolution imaging has to be performed on the top areas of the deformable cell. Moreover the topographical characteristic for the living cells, i.e. their doughnut shape, gives one little chance to find a flat non-tilted area. Hence in most cases we are scanning significantly curved surfaces. This fact, together with the high tendency of the soft membrane for deformation due to the interaction with the harder tip, are the most important reasons why it is difficult to obtain images of red blood cells and why the image resolution is not high.

In the light of the above discussion it is not surprising that it is easier to obtain high resolution images of the membrane in swollen cells. Fig. 3 presents the results obtained for such cells using a standard AFM tip. Fig. 3A is an image of a whole cell, whilst Fig. 3B is a magnified version of the bottom left hand corner of the cell. At this magnification some texturing of the cell is clear. A lattice consisting of apparently randomly distributed and linked linear,

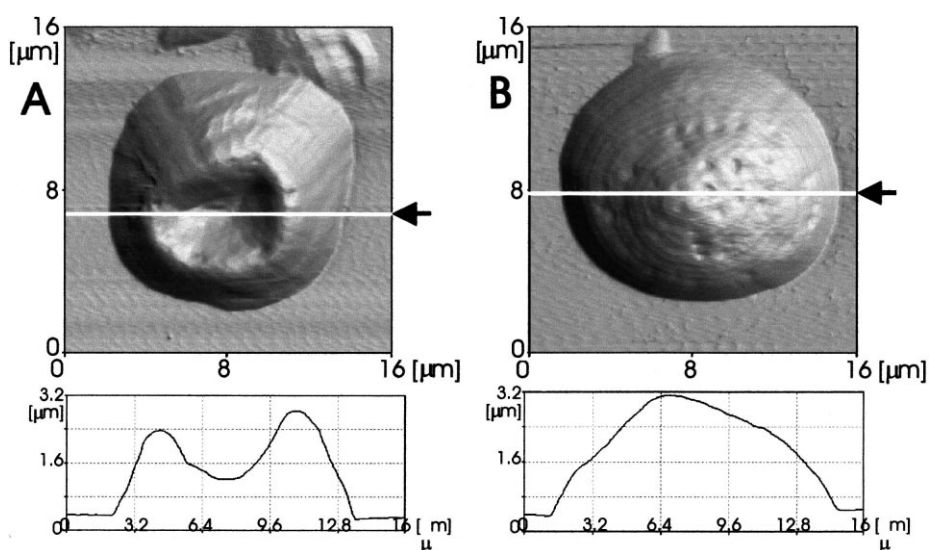


Fig. 2. AFM images and surface profiles obtained for (A) biconcave shaped cell and (B) swollen cell in PBS solution; scanning area $16 \times 16 \mu\text{m}^2$, max. height $3.2 \mu\text{m}$.

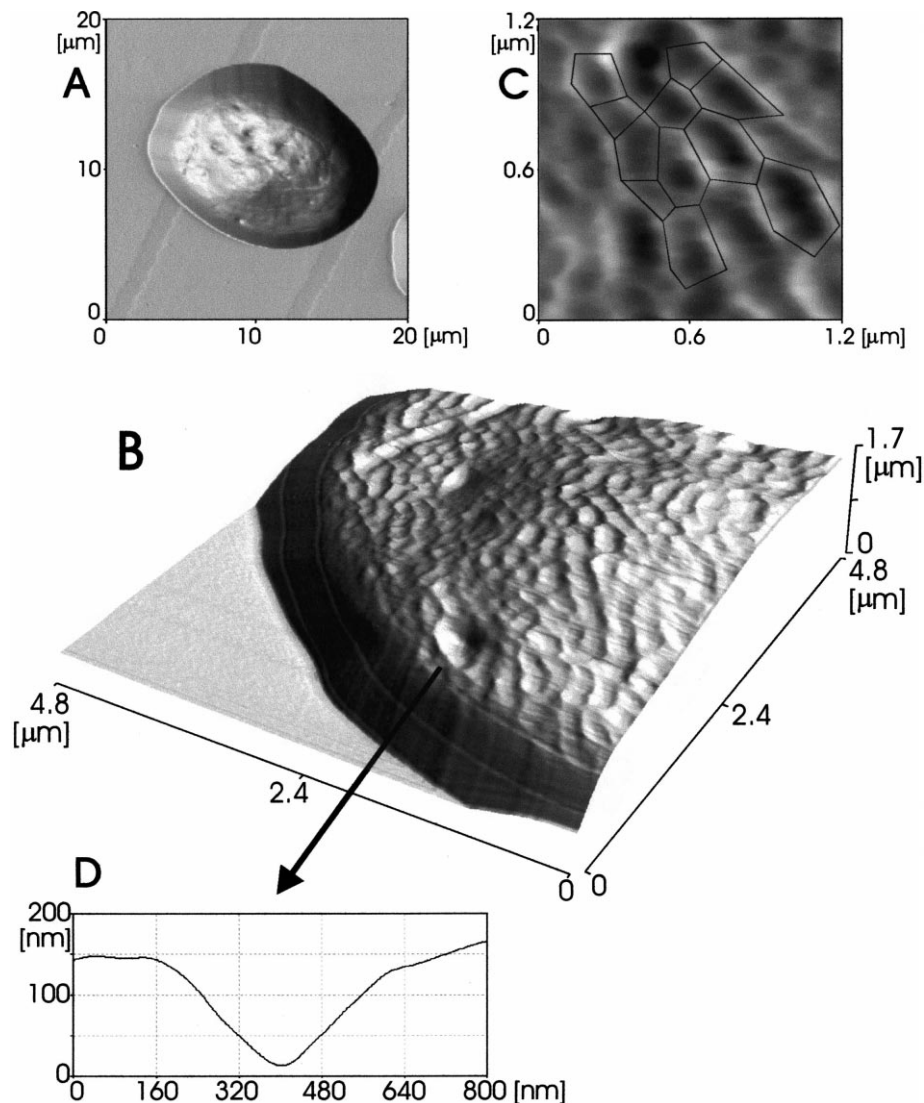


Fig. 3. AFM image of swollen cell in PBS solution. (A) Image of whole cell; scanning area $12 \times 12 \mu\text{m}^2$, max. height $2.5 \mu\text{m}$. (B) Three-dimensional representation of left hand quarter of cell showing texturing of the cell surface; scanning area $4.8 \times 4.8 \mu\text{m}^2$, max. height $1.7 \mu\text{m}$. (C) Non-processed image of further enlargement of surface texturing (additional network of black lines linking high areas is added as a guide to the eye); scanning area $1.2 \times 1.2 \mu\text{m}^2$, max. height change 30 nm . (D) Cross-section through one of the surface dimples observed on the cell surface.

pentagonal and hexagonal subunits can clearly be observed. Fig. 3C is a further enlargement. From this non-processed image the light areas are regions of high material and the dark areas are ‘valleys’. Additional lines, which link high areas, have been added to guide the eye. The dimensions of these ridges are of the order $100\text{--}250 \text{ nm}$ in length, $10\text{--}20 \text{ nm}$ in height, and $50\text{--}70 \text{ nm}$ in width, although this may well be an overestimate of the width due to broadening out the ridge by the shape of the tip, as

discussed above. At this point it is worth remembering how an AFM works. An AFM image is one constant interaction between the tip and substrate. If the substrate is of constant compliance, then this corresponds to a surface topography. It is important to note that during study of materials of different compliance, the apparent topography of the surface cannot correspond to the real topography and is modulated by the local compressibility of the sample. Thus, when the surface is comprised of a harder

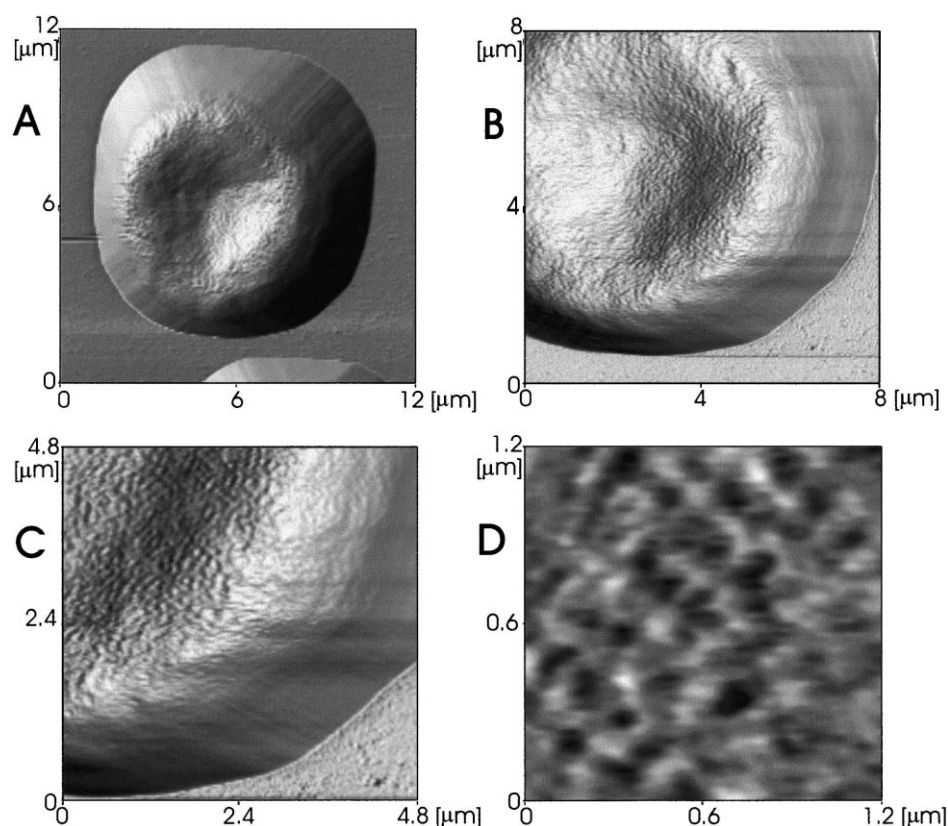


Fig. 4. AFM image of doughnut shaped cell in PBS solution. (A) Image of whole cell; scanning area $12 \times 12 \mu\text{m}^2$, max. height $2 \mu\text{m}$; (B,C) enlargements of the same part of the cell; scanning area: (B) $8 \times 8 \mu\text{m}^2$, (C) $4.8 \times 4.8 \mu\text{m}^2$, max. height $1.7 \mu\text{m}$; (D) non-processed image of further enlargement of surface, scanning area $1.2 \times 1.2 \mu\text{m}^2$, max. height change 20 nm .

material and a soft material, the image will still be one of constant tip surface interaction, such that the hard areas will appear to be high areas on the substrate. This is the case here. The texturing observed is entirely consistent with this being due to the underlying cytoskeleton of the cell [19]. In a red blood cell this protein layer consisting primarily of spectrin lies under the surface of the cell membrane and is attached to the membrane every 200 nm or so. This corresponds to the length of the ridges observed in Fig. 3B,C. Moreover, transmission electron microscopy has revealed that frequently the spectrin is joined to form approximately tessellated pentagonal and hexagonal structures, these are clearly observed in various regions of Fig. 3B,C. Fig. 3D is a cross-section through one of the dimples on the surface characteristic for the swollen cell. The dimple has a diameter of some 400–500 nm (note again that this cross-sectional profile is distorted by the tip shape to some extent) and a depth of 100 nm. Therefore, this

dimple may be due to one of the anchoring points of the cytoskeleton to the integral proteins of the plasma membrane being broken, such that the AFM tip pushes further into the cell than if the cytoskeleton were attached to the erythrocyte membrane at that point [20,21].

As previously mentioned the study of a doughnut shaped cell is more difficult. Using standard AFM tips we could not observe any detailed structure of these cells. These difficulties result from the interaction of the sides of the broad standard AFM tip. Hence standard tips slide down from this surface and do not respond to the surface morphology. In our experiments detailed structures of the cells become visible only using 'super tips' which are characterised by their slender shape, i.e. higher value of height/width ratio (aspect ratio) of the end of the tip 10:1 (instead of 1.1:1 calculated for standard tip). The results are collected in Fig. 4. Fig. 4A is an image of a whole cell, whilst Fig. 4B–D are the cor-

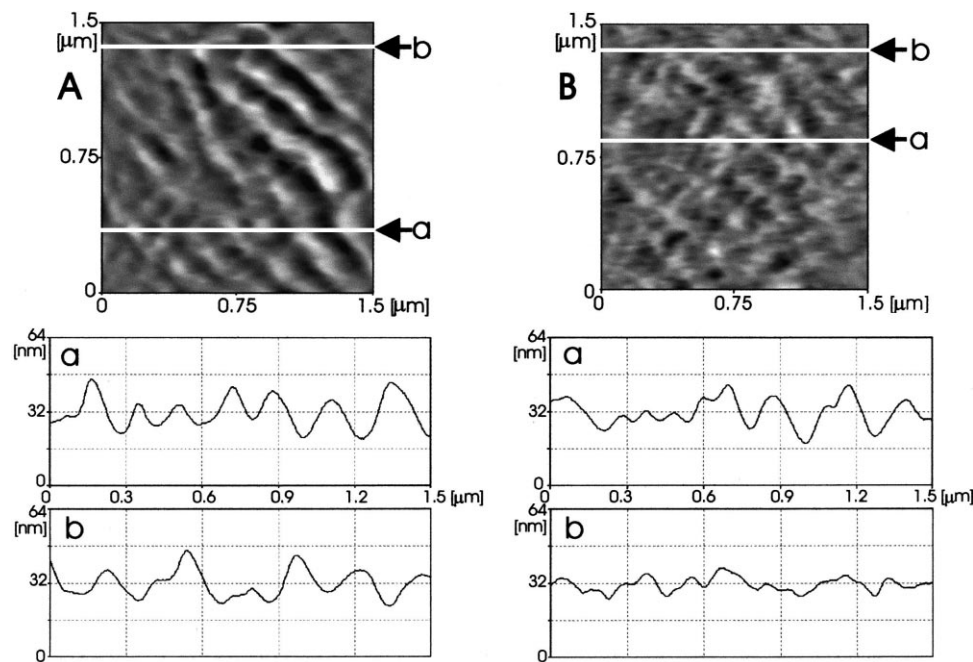


Fig. 5. Comparison of the AFM images and corresponding surface profiles obtained in PBS solution for (A) swollen and (B) doughnut shaped erythrocytes. AFM images: scanning area $1.5 \times 1.5 \mu\text{m}^2$, max. height 30 nm.

responding magnifications. The structure of the cell is visible on the upper surface of the cell in spite of the tilt on the internal sides of the cell. In contrast to the results presented for swollen cells, in this case no dimples are observed, suggesting that the underlying cytoskeleton is not broken and is well anchored to the integral proteins of the plasma membrane. For both swollen and doughnut cells, the structure is similar and is characterised by the lattice corresponding to the underlying protein network. However, a more detailed examination of these structures reveals an interesting difference. A comparison of line scans from randomly chosen sites from two kinds of cells is presented in Fig. 5. Five randomly selected profiles were analysed for each cell. Two of them are shown for each cell in Fig. 5. The surface of the doughnut cell (Fig. 5B) exhibits three different levels. From the middle level, which corresponds to the grey areas of the image, many ledges are observed as white dots on the image. The thickness of the ledges is a few nm, which implies that these areas may correspond to the stiffer membrane proteins that protrude from the surface of the membrane [11]. Many gaps are observed as the centre part of each subunit of the lattice. This lower level corresponds to the black areas of the image and, as was the case for the 'swollen cells',

the areas in the middle of the protein lattice units are more compliant than the areas directly above the protein network. Thus in these places the AFM tip enters the membrane deeper and consequently produces the observed 'holes'. It is interesting to compare the average size of the lattice subunits observed for two different cells. The average distance between peaks calculated for each profile for doughnut cells varies between 100 and 150 nm, whilst the corresponding distance calculated for swollen cells is larger and varies between 180 and 220 nm (Fig. 5A). However, it is possible to find areas on the doughnut cell very similar to those observed on the swollen cell (right part of profile a in Fig. 5B). There are two possible explanations for this observation. One could speculate that in the round cell the spectrin is attached to the plasma membrane at fewer points and so the mean separation between the peaks is higher. Alternatively the observed differences in lattice size may result from the stretching of the network which is expected for the swollen cell.

Here it is interesting to speculate on the mechanism by which internal features of cells such as those observed here can be observed using AFM. Henderson [4] has proposed two possibilities. In one case the plasma membrane may conform to the underlying

rigid structural elements. In this mechanism the scanning tip simply follows the contour of the membrane. However, a second possibility is that the tip directly penetrates the membrane during imaging and makes direct contact with the harder structures below. A further mechanism is also possible, where the tip presses the membrane during scanning and deforms it so that the cantilever follows the contours of the underlying cytoskeleton. If the first mechanism were correct then the internal structure of cytoskeleton on the cell surface would be observed by other methods, for example scanning electron microscopy. Since this is not the case, this mechanism is unlikely to be the case here. However, it is impossible to determine which of the other two mechanisms is occurring.

Acknowledgements

R. Nowakowski thanks the Royal Society for financial support according to the Royal Society Postdoctoral Fellowship Programme. The experiments comply with the current laws of the UK.

References

- [1] H.-J. Butt, E.K. Wolff, S.A.C. Gould, B. Dixon Northern, C.M. Peterson, P.K. Hansma, Imaging cells with the atomic force microscope, *J. Struct. Biol.* 105 (1990) 54–61.
- [2] S.A.C. Gould, B. Drake, C.B. Prater, A.L. Weisenhorn, S. Manne, H.G. Hansma, P.K. Hansma, J. Missie, M. Longmire, V. Elings, B. Dixon Northern, B. Mukerjee, C.M. Peterson, W. Stoeckenius, T.R. Albrecht, C.F. Quate, From atoms to integrated circuit chips, blood cells, and bacteria with the atomic force microscope, *J. Vac. Sci. Technol. A* 8 (1990) 369–373.
- [3] H.G. Hansma, J.H. Hoh, Biomolecular imaging with the atomic force microscope, *Annu. Rev. Biophys. Biomol. Struct.* 23 (1994) 115–139.
- [4] E. Henderson, Imaging of living cells by atomic force microscopy, *Prog. Surf. Sci.* 46 (1994) 39–60.
- [5] L. Ratneshwar, A.J. Scott, Biological applications of atomic force microscopy, *Am. J. Physiol. Cell Physiol.* 266 (1994) C1–C21.
- [6] H.G. Hansma, Atomic force microscopy of biomolecules, *J. Vac. Sci. Technol. B* 14 (1996) 1390–1394.
- [7] E. Henderson, P.G. Haydon, D.S. Sakaguchi, Actin filament dynamics in living glial cells imaged by atomic force microscopy, *Science* 257 (1992) 1944–1946.
- [8] D. Braunstein, A. Spudich, Structure and activation dynamics of RBL-2H3 cells observed with scanning force microscopy, *Biophys. J.* 66 (1994) 1717–1725.
- [9] L. Chang, T. Kious, M. Yorgancioglu, D. Keller, J. Pfeiffer, Cytoskeleton of living, unstained cells imaged by scanning force microscopy, *Biophys. J.* 64 (1993) 1282–1286.
- [10] J.H. Hoh, C.-A. Schoenenberger, Surface morphology and mechanical properties of MDCK monolayers by atomic force microscopy, *J. Cell Sci.* 107 (1994) 1105–1114.
- [11] J. Viitala, J. Järnefelt, The red cell surface revisited, *Trends Biochem. Sci.* 1995 (1985) 392–395.
- [12] A. Elgsaeter, B.T. Stokke, A. Mikkelsen, D. Branton, The molecular basis of erythrocyte shape, *Science* 234 (1986) 1217–1223.
- [13] R.M. Hochmuth, R.E. Waugh, Erythrocyte membrane elasticity and viscosity, *Annu. Rev. Physiol.* 49 (1987) 209–219.
- [14] B.W. Shen, Ultrastructure and function of membrane skeleton, in: P. Agree, J.C. Parker (Eds.), *Red Blood Cell Membranes: Structure, Function, Clinical Implications*, Marcel Dekker, New York, 1989, pp. 261–297.
- [15] S. Chien, L.A. Sung, Molecular basis of red cell membrane rheology, *Biorheology* 27 (1990) 327–344.
- [16] V. Bennett, D.M. Gilligan, The spectrin-based membrane skeleton and micron-scale organization of the plasma membrane, *Annu. Rev. Cell Biol.* 9 (1993) 27–66.
- [17] W. Häberle, J.K.H. Horber, G. Binnig, Force microscopy on living cells, *J. Vac. Sci. Technol. B* 9 (1991) 1210–1213.
- [18] J.M. Mikrut, R.C. MacDonald, Analysis of red blood cell cytoskeleton using an atomic force microscope, *Am. Biotechnol. Lab.* 12 (1994) 26.
- [19] S.-L. Liu, L.H. Derick, J. Palek, Visualization of the hexagonal lattice in the erythrocyte membrane skeleton, *J. Cell Biol.* 104 (1987) 527–536.
- [20] H.S. Jacob, Pathologic states of the erythrocyte membrane, in: G. Weissmann, R. Claiborne (Eds.), *Cell Membranes Biochemistry. Cell Biology and Pathology*, HP Publ. Co., New York, 1975, pp. 249–255.
- [21] C.A. Smith, E.J. Wood, The erythrocyte cytoskeleton, in: C.A. Smith, E.J. Wood (Eds.), *Cell Biology*, 2nd edn., Chapman and Hall, London, 1996, pp. 244–245.